



Spirocyclic, macrocyclic and ladder complexes of coinage metals and mercury with dichalcogeno P₂N₂-supported anions

Journal:	<i>Dalton Transactions</i>
Manuscript ID:	DT-ART-01-2015-000159.R1
Article Type:	Paper
Date Submitted by the Author:	05-Feb-2015
Complete List of Authors:	Chivers, Tristram; The University of Calgary, Department of Chemistry Nordheider, Andreas; University of St Andrews, Chemistry athukorala arachchige, Kasun; University of St Andrews, Department of Chemistry Slawin, Alexandra; University of St Andrews, Chemistry Thirumoorthi, Ramalingam; University of Calgary, Chemistry Woollins, J; University of St Andrews, Department of Chemistry Huell, Katharina; University of St Andrews, Chemistry

ARTICLE

Spirocyclic, macrocyclic and ladder complexes of coinage metals and mercury with dichalcogeno P₂N₂-supported anions

Andreas Nordheider,^{a,b} Katharina Hüll,^a Kasun S. Athukorala Arachchige,^a Alexandra M. Z. Slawin^a, J. Derek Woollins,^a Ramalingam Thirumoorthy^b and Tristram Chivers^{b*}

In memory of Professor Kenneth Wade

Metathetical reactions of alkali-metal derivatives of the dianion [^tBuN(Se)P(μ-N^tBu)₂P(Se)N^tBu]²⁻ (**2Se²⁻**) with Ag(NHC)Cl, Ag[BF₄], AuCl(THT) and HgCl₂, as well as the reaction of **2S²⁻** with AuCl(THT) were investigated. The observed products all incorporate the monoprotonated ligands **2SeH⁻** or **2SH⁻** in a variety structural arrangements around the metal centres, including tetrameric and trimeric macrocycles [Ag and Au (E = Se)], a ladder (Au, E = S) and a spirocycle (Hg); the ladder contains both the dianion **2S²⁻** and the monoanion **2SH⁻** as ligands linking three Au₂ units. All complexes have been characterised in the solid state by single crystal X-ray analyses and in solution by multinuclear (¹H, ³¹P and ⁷⁷Se) NMR spectra.

Cite this: DOI: 10.1039/x0xx00000x

Received 00th January 2012,
Accepted 00th January 2012

DOI: 10.1039/x0xx00000x

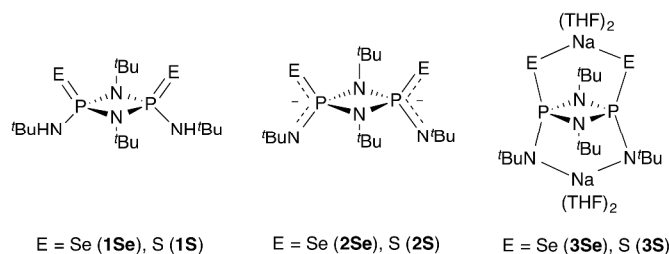
www.rsc.org/

Introduction

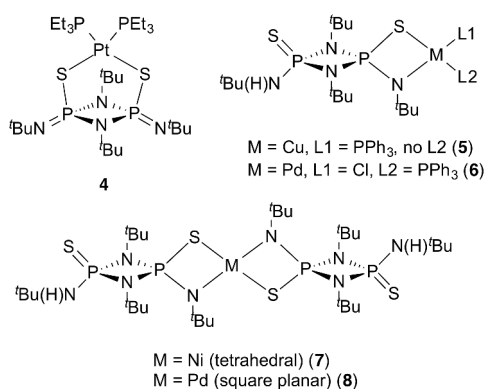
Four-membered rings of the type [XP(μ-NR)]₂ (known as cyclodiphosph(III)azanes) occupy a prominent position in the long and venerable history of inorganic ring systems.^{1,2} The incorporation of P₂N₂ rings as building blocks in macrocycles has been a significant feature of recent investigations of these heterocycles. For example, Wright *et al.* have generated cyclic oligomers with bridging amido groups that are able to encapsulate halide ions suggesting applications in host-guest chemistry.³ The same group has also characterised P₂N₂ macrocycles with bridging chalcogen (E) atoms, including a tetramer (E = O)⁴ and a hexamer (E = Se);⁵ the P atoms in the latter are in different formal oxidation states (III and V). More recently, Balakrishna *et al.* have reported intriguing Cu₄X₄ (X = Br, I) clusters with *cyclo*-P₂N₂ linkers that resemble a sodalite framework.⁶ Balakrishna has also described functionalised P₂N₂ macrocycles with gold-bridges that incorporate a ClO₄⁻ ion.⁷

The P(III)/P(III) systems with terminal alkylamido groups are readily oxidised by selenium or sulfur to give the corresponding P(V)/P(V) heterocycles, *e.g.* [^tBuNH(E)P(μ-N^tBu)]₂ (**1Se** and **1S**).⁸ In 2000 we showed that deprotonation of the neutral precursors **1Se** and **1S** produces the corresponding

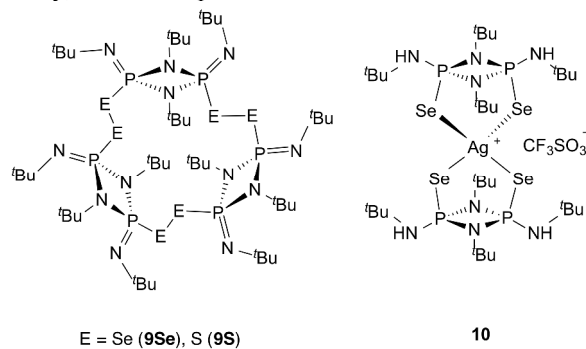
dianions **2Se²⁻** and **2S²⁻** as alkali-metal reagents, *e.g.* the disodium derivatives **3Se** and **3S**.⁹



The coordination chemistry of the multidentate dianions **2Se²⁻** and **2S²⁻** is potentially versatile owing to the presence of two hard (N) and two soft (S) donor sites.⁸ In preliminary studies we showed that Pt(II) engages in *S,S'*-coordination to **2S²⁻** in the complex **4**.^{9b} Those investigations also revealed that metathesis of the monoprotonated monoanion **2SH⁻** with Cu(I), Ni(II) and Pd(II) reagents produces the *N,S*-bonded complexes **5-8** with a spirocyclic metal centre in the case group of 10 metals (**7** and **8**).^{9b}



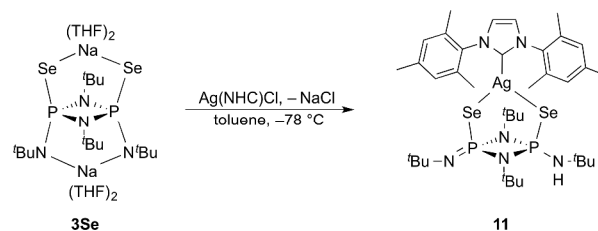
In more recent work we demonstrated that two-electron oxidation of the dianions 2Se^{2-} and 2S^{2-} with I_2 generates trimeric macrocycles with a planar P_6E_6 framework **9Se** and **9S**, respectively.¹⁰ Although the cavity of the ring in **9Se** and **9S** is too small to accommodate metal ions, we were inspired by the reports of Krossing *et al.* on the stabilisation of selenium homocycles, *cyclo*- Se_6 , $-\text{Se}_{12}$ and $-\text{Se}_{19}$, in Cu(I) and Ag(I) complexes¹¹ to investigate the coordination behaviour of **9Se** in the presence of coinage metals, including possible ring transformations. However, the treatment of **9Se** with silver(I) triflate $\text{Ag}[\text{CF}_3\text{SO}_3]$ produced the ionic compound $[\text{Ag}(\mathbf{1Se})_2][\text{CF}_3\text{SO}_3]$ (**10**) in which the cation is a complex of Ag^+ with two neutral ligands **1Se**.¹² In the light of this result we decided to take a different approach to the synthesis of macrocycles incorporating $\text{P}_2\text{N}_2\text{E}_2$ building blocks and coinage metals, namely metathetical reactions of **3Se** and **3S** with various M(I) reagents ($M = \text{Ag}, \text{Au}$). In this contribution the geometrical influence of the coinage metal is evaluated through reactions of **3Se** with $\text{Ag}(\text{NHC})\text{Cl}$, $\text{Ag}[\text{BF}_4]$ and $\text{AuCl}(\text{THT})$. In view of the additional information available from NMR spectra of selenium-containing compounds (^{77}Se , $I = 1/2$, 7.6%), the emphasis of these studies has been on reactions of **3Se**. However, the consequence of changing the chalcogen was also assessed *via* an examination of the reaction of **3S** with $\text{AuCl}(\text{THT})$. Finally, the outcome of the reaction of **3Se** with HgCl_2 , as an example of a divalent metal that favours linear geometry, was also explored.



Results and discussion

Synthesis, X-ray structures and NMR spectra of silver complexes of 2SeH^-

The reaction of **3Se** with the *N*-heterocyclic carbene (NHC) complex $\text{Ag}(\text{NHC})\text{Cl}$ produces the metallocycle $[(\text{tBuNP}(\mu\text{-N}^t\text{Bu})_2\text{PN}(\text{H})^t\text{Bu})(\mu\text{-SeAg}(\text{NHC})\text{Se})]$ (**11**) in 12% yield (Scheme 1), accompanied by the diprotonated derivative **1Se** as a by-product.^{9,13}



Scheme 1 Synthesis of the Ag(I) complex **11**.

A crystal structure of **11** was obtained after recrystallisation from *n*-hexane at $-40\text{ }^\circ\text{C}$. As illustrated in Fig. 1, the complex is comprised of the monoanionic ligand 2SeH^- , which is *Se, Se'*-coordinated to the $[(\text{NHC})\text{Ag}]^+$ cation.

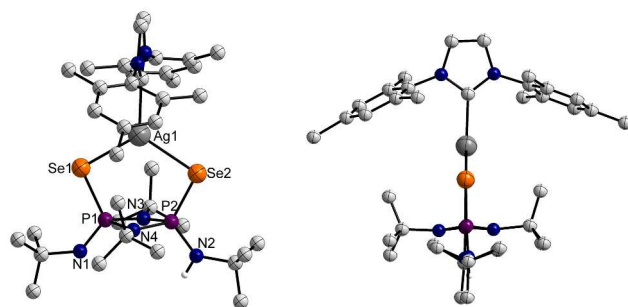


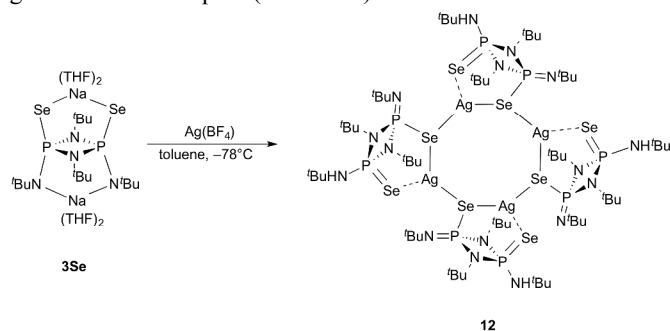
Fig. 1 Molecular structure of **11** shown from perpendicular views. Hydrogen atoms bonded to C atoms are omitted for clarity. Selected bond lengths (Å) and angles ($^\circ$): Ag1-Se1 2.6067(17), Ag1-Se2 2.6356(17), Ag1-C21 2.129(11), Se1-P1 2.166(3), Se2-P2 2.131(3), P1-N1 1.565(9), P1-N3 1.699(7), P1-N4 1.687(8), P2-N2 1.596(8), P2-N3 1.690(8), P2-N4 1.681(8), Se1-Ag1-Se2 116.81(4), Se1-Ag1-C21 122.6(4), Se2-Ag1-C21 120.6(4), Ag1-Se1-P1 95.28(8), Ag1-Se2-P2 94.27(9).

The P-Se-Ag-Se-P ring in **11** is almost planar with the P_2N_2 ring perpendicular to this plane. The Ag-Se bond lengths (range 2.607(2)–2.635(2) Å) are comparable to the shorter bonds in the related complex $[\text{Ag}(\text{Ph}_2\text{P}(\text{Se})\text{NHP}(\text{Se})\text{Ph}_2)_2][\text{BF}_4]$ (2.634(2)–2.713(3) Å).¹⁴ The P-Se bond lengths of 2.131(3) Å and 2.166(3) Å (*cf.* 2.078(1)–2.070(1) Å for the diprotonated ligand **1Se**)¹⁵ indicate significant double bond character. As expected, the P-N_{exo} bond distance of 1.601(8) Å involving the protonated nitrogen atom N2 is significantly longer than the value of 1.562(9) Å found for P1-N1 [*cf.* 1.501(7)–1.507(8) Å for the exocyclic P=N bonds in **9Se**]. The geometry around Ag1 is slightly distorted from trigonal planar ($\Sigma\angle\text{Ag1} = 360^\circ$, range 116.8–122.8 $^\circ$).

The ^{31}P NMR spectrum of **11** at 25 $^\circ\text{C}$ exhibits two well-separated resonances at 13.8 ppm ($^1J(\text{P}, \text{Se}) \approx 714$ Hz) and

–34.1 ppm ($^1J(\text{P},\text{Se}) \approx 650$ Hz), suggesting that the crystallographic inequivalence of P1 and P2 observed in the solid state is maintained in solution. These signals are tentatively assigned to P1 and P2, respectively, from a consideration of the relative $^1J(\text{P},\text{Se})$ and $d(\text{P}–\text{Se})$ values (the shorter bond should give the larger coupling constant). However, these resonances are broad, presumably reflecting the existence of rapid exchange equilibria.¹⁶ The ^{77}Se NMR spectrum of **11** exhibits two doublets at 65.5 ppm ($^1J(\text{Se},\text{P}) \approx 647$ Hz) and –62.8 ppm ($^1J(\text{Se},\text{P}) \approx 722$ Hz), respectively.

By contrast to the outcome of the reaction of **3Se** with $\text{Ag}(\text{NHC})\text{Cl}$, the treatment of the silver(I) salt $\text{Ag}[\text{BF}_4]$ with **3Se** in toluene at -78°C gave rise to an eight-membered ring with alternating Ag and Se atoms (**12**) in which the monoanionic ligands 2SeH^- balance the charge of Ag^+ ions to give a neutral complex (Scheme 2).



Scheme 2 Synthesis of the eight-membered Ag_4Se_4 ring **12**.

Crystals of the tetramer $\{\text{Ag}\{\mu\text{-}^i\text{Bu}(\text{H})\text{N}(\text{Se})\text{P}(\mu\text{-}\text{N}^i\text{Bu})_2\text{P}(\text{Se})\text{N}^i\text{Bu}\}_4\}$ (**12**) were isolated after recrystallisation of the compound in *n*-hexane at -40°C . The molecular structure is illustrated in Fig. 2 together with selected geometrical parameters.

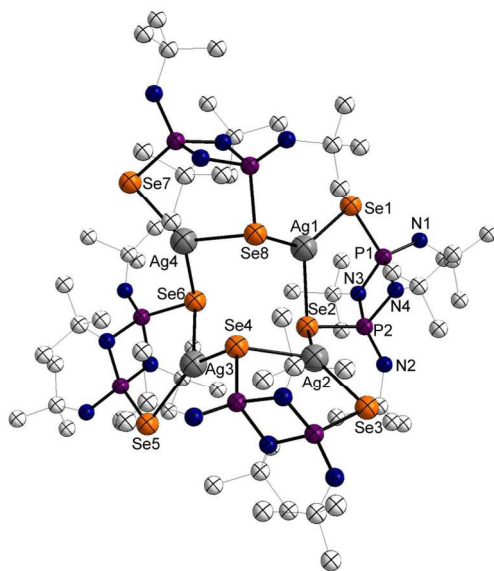


Fig. 2 Molecular structure of **12**. Hydrogen atoms omitted for clarity. Selected bond lengths (Å) and angles ($^\circ$) (data shown are limited to those involving Ag1 as representative of the four

crystallographically inequivalent Ag atoms): Ag1–Se1 2.6197(17), Ag1–Se2 2.6450(16), Ag1–Se8 2.5692(16), Se1–P1 2.154(4), Se2–P2 2.229(3), P1–N1 1.629(11), P2–N2 1.515(12); Se1–Ag1–Se2 116.76(5), Se1–Ag1–Se8 134.39(6), Se2–Ag1–Se8 108.59(5).

In the polycyclic complex **12** the ligands 2SeH^- fulfil a bridging role *via* the three-coordinate selenium atoms, which form the central Ag_4Se_4 ring; the selenium atoms outside this ring are two-coordinate. In this respect the structure is comparable to those of the oligomeric silver(I) complexes $\{\text{Ag}[\text{N}(\text{Pr}_2\text{P}\text{Te}_2)]_6\}$ and $\{\text{Ag}[\text{N}(\text{Ph}_2\text{P}\text{Te}_2)]_4\}$ which incorporate Ag_6Te_6 and Ag_4Te_4 rings, respectively, and bridging, acyclic monoanionic ligands $[(\text{TePR}_2)_2\text{N}]^-$.¹⁷ The silver centres in all three compounds are each bound to two-coordinate chalcogen centres from one ligand and one bridging, three-coordinate chalcogen from an adjacent ligand. As illustrated in Fig. 3, the eight-membered ring in **12** exhibits a C-shaped zigzag arrangement.

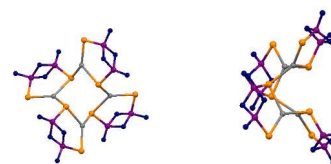


Fig. 3 Two views of the Ag_4Se_4 ring in **12** (C and H atoms omitted for clarity).

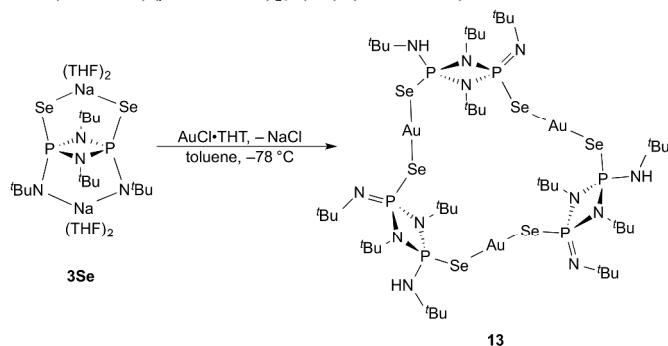
The Ag–Se bond lengths in **12** are in the range 2.561(2)–2.647(2) Å, but there is no correlation between these values and the coordination number (2 or 3) of the Se atoms. The values do, however, indicate stronger coordination of the monoanionic ligands 2SeH^- to Ag^+ compared to that in **11** ($d(\text{Ag}–\text{Se}) = 2.714(2)$ – $2.741(2)$ Å). In contrast, the expected correlation of bond length with coordination number does pertain for the values of $d(\text{P}–\text{Se})$. For the three-coordinate Se atoms (Se2,4,6,8) the P–Se distances range from 2.222(3) to 2.229(3) Å, (*cf.* 2.253(2)–2.262(2) Å for the trimeric macrocycle **9Se**), whereas the two-coordinate centres Se1,3,5,7 show significantly shorter P–Se distances of 2.146(4)–2.154(4) Å, closer to formal double-bond values (*cf.* $d(\text{P}=\text{Se}) = 2.070(1)$ – $2.078(1)$ Å for **1Se**).¹⁵ Compared to the monomeric structure of **11**, the incorporation of Ag in an eight-membered ring effects a substantial distortion from trigonal geometry in **12** ($\Sigma\angle\text{Ag1} = 359.8^\circ$, range 108.6–134.4 $^\circ$).

The ^{31}P NMR spectrum of **12** in toluene exhibits two well-separated broad singlets at 13.9 and –55.4 ppm for the two phosphorus environments of the 2SeH^- ligands. However, the $^1J(\text{Se},\text{P})$ values could not be discerned owing to the broadness of the resonances, which may be the result of a rapid (proton) exchange process.¹⁶ Unfortunately, low temperature could not be acquired owing to the poor solubility of **11** and **12**.

Synthesis, X-ray structures and NMR spectra of a trimeric gold(I) macrocycle

We next turned our attention to the reactions of the dianionic reagents **3Se** with $\text{AuCl}(\text{THT})$ in order to evaluate the influence

of the coinage metal on the structural arrangement in the resulting complexes. Interestingly, the treatment of **3Se** with one equivalent of AuCl(THT) produced a bright red compound identified as the trimeric metallocycle $[(^t\text{BuNP}(\mu\text{-N}^t\text{Bu})_2\text{P}^t\text{BuN})(\mu\text{-SeAuSe})_3]$ (**13**) (Scheme 3).



Scheme 3 Synthesis of the trimeric Au(I) macrocycle **13**.

The crystal structure of **13** was elucidated after recrystallisation of the compound in *n*-hexane at $-40\text{ }^\circ\text{C}$, which yielded pink prism-shaped crystals (Fig. 4). As was the case for **11** and **12**, the monoprotonated ligands 2SeH^- in **13** balance the charge of the Au^+ centres giving an overall neutral macrocycle.

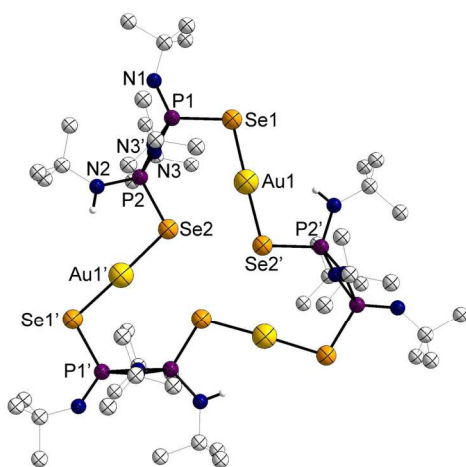


Fig. 4 Molecular structure of the trimeric Au(I) complex **13**. Hydrogen atoms bonded to C atoms are omitted for clarity. Selected bond lengths (Å) and angles ($^\circ$): Au1–Se1 2.396(2), Au1–Se2 2.4189(17), Se1–P1 2.221(3), Se2–P2 2.173(5), P1–N1 1.519(15), P2–N2 1.616(9); Se1–Au1–Se2 178.30(5), Au1–Se1–P1 103.81(12), Au1–Se2–P2 105.77(9).

The gold-containing macrocycle **13** is closely related to the previously reported trimer **9Se** by the formal insertion of Au atoms into the three Se–Se bonds of the latter, except that none of the exocyclic nitrogen centres are protonated in the “gold-free” ring. The different structure-directing influence of the coinage metals in **12** and **13** is noteworthy. In contrast to the trigonal coordination exhibited by the Ag^+ ions in **12**, the Se–Au–Se units in **13** are essentially linear ($\angle(\text{Se–Au–Se}) = 178.30(5)^\circ$) with almost equal Au–Se bond lengths of 2.396(2) and 2.419(2) Å. The $\text{Au}_3\text{Se}_6\text{P}_6$ framework in **13** is planar with

the P_2N_2 rings perpendicular to this plane, as observed for **9Se**.¹⁰ The markedly different P–N bond lengths for the exocyclic nitrogen atoms in **13**, ($d(\text{P–N}) = 1.616(9)$ Å and 1.519(15) Å), clearly reflect the protonation of one of these centres.

Examples of trinuclear gold(I) metallatriangles are widespread and they invariably exhibit intramolecular Au⋯Au interactions of ca. 3.0–3.2 Å.¹⁸ An intriguing recent representative, the trimeric dithiophosphate complex $[\text{Au}_2\text{S}_2\text{P-1,4-C}_6\text{H}_4\text{OEt}_2(\text{trans-1,2-O,O'-C}_6\text{H}_{10})_3]$ embodies distances of 3.28–3.31 Å within the Au_3 triangle and luminesces in the solid state at room temperature.¹⁹ By contrast, the Au⋯Au distances in **13** are 5.752 Å, *cf.* sum of van der Waals radii for Au = 3.80 Å.²⁰

Although complexes with linear Se–Au–Se scaffolds are not unusual,²¹ five-atom P–Se–Au–Se–P arrangements are scarce, *e.g.* the Au(I) complex $[(\text{Ph}_3\text{PSe})_2\text{Au}][\text{SbF}_6]$ which exhibits a Se–Au–Se angle of $172.6(1)^\circ$.²² The Au–Se bond lengths of 2.396(2)–2.419(2) Å in **13** are comparable to the corresponding values of 2.390(1)–2.395(1) Å observed for the latter complex.²² The P–Se distances of 2.173(5) Å and 2.221(3) Å are similar to those reported for **9Se** (2.253(2)–2.262(2) Å)¹⁰ and $[(\text{Ph}_3\text{PSe})_2\text{Au}][\text{SbF}_6]$ (2.173(1)–2.174(1) Å).²²

The ^{31}P NMR spectrum of **13** in toluene exhibits two doublets at 4.9 ppm ($^2J(\text{P,P}) = 16.4$ Hz; $^1J(\text{P,Se}) \approx 657$ Hz) and -57.6 ppm ($^2J(\text{P,P}) = 16.4$ Hz; $^1J(\text{P,Se}) \approx 627$ Hz). By contrast, only one resonance was observed in the ^{31}P NMR spectrum of the “gold-free” trimer **9Se** in solution (however, two signals were evident in the solid-state spectrum, consistent with the crystallographic inequivalence of the P atoms of the P_2N_2 rings in **9Se**).¹⁰ This observation indicates that, in contrast to **9Se**, the gold complex **13** does not undergo fluxional behaviour leading to equivalence of the different phosphorus environments on the NMR time scale in solution. Consistently, the ^{77}Se NMR spectrum of **13** in toluene reveals two well-separated resonances at 132.4 ppm ($^1J(\text{P,Se}) \approx 621$ Hz) and 209.0 ppm ($^1J(\text{P,Se}) \approx 644$ Hz).

The space-filling model of **13** (Fig. 5) shows only a small cavity in the centre of the macromolecule; the transannular Se1⋯Se1' distance is 3.545 Å in **13**, *cf.* 3.315 Å in **9Se**.¹⁰ For comparison, the folded conformation of the tetrameric silver(I) metallocycle **12** (Fig. 3) exhibits a range of transannular Se⋯Se distances (3.686, 4.184 and 4.778 Å), the shortest of which provides inadequate room for the entrapment of small anions (Fig. 5).

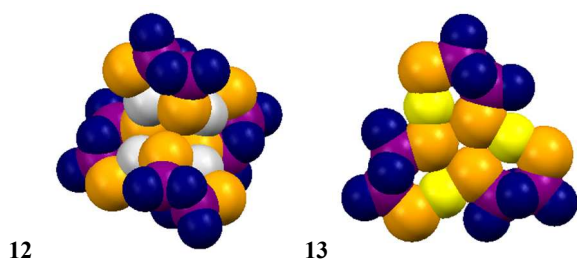
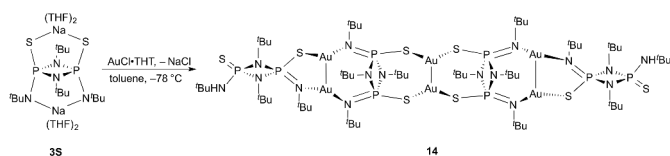


Fig. 5 Space-filling models of **12** and **13**; H and C atoms are omitted.

Synthesis, X-ray structure and NMR spectra of a ladder with three Au₂ units

In order to determine the effect of changing the chalcogen on the nature of the gold complex formed, the reaction of the sulfur reagent **3S** with AuCl(THT) was investigated. A colourless product, which was shown to have a unique twisted ladder-like structure (**14**, Scheme 4) was isolated in 49 % yield; the diprotonated precursor **1S** was identified as a minor by-product in the ³¹P NMR spectrum of the reaction mixture.²³



Scheme 4 Synthesis of the ladder complex **14** incorporating three Au₂ units.

Colourless crystals suitable for a single crystal X-ray analysis were isolated after recrystallisation of **14** from *n*-hexane at $-40\text{ }^{\circ}\text{C}$. The molecular structure is illustrated in Fig. 6a, which also gives selected geometrical parameters.

a)

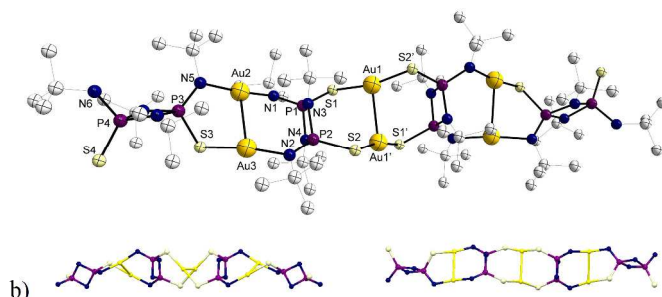


Fig. 6 (a) Molecular structure of the gold complex **14**. Hydrogen atoms omitted for clarity, but the N6 atoms are protonated (b) two views of the ladder arrangement of Au₂ units in **14**. Selected bond lengths (Å) and bond angles ($^{\circ}$): Au1–Au1' 2.8737(7), Au2–Au3 3.002, Au1–S1 2.291(2), Au1–S2 2.289(2), Au2–N1 2.047(6), Au2–N5 2.073(6), Au3–S3 2.288(2), Au3–N2 2.082(6), S1–P1 2.036(3), S2–P2 2.040(3),

S3–P3 2.036(3), S4–P4 1.929(3), P3–N5 1.596(7), P4–N6 1.642(7); \angle S1–Au1–S2 = 167.4(1), N1–Au2–N5 = 171.1(2), S3–Au3–N2 = 172.0(2).

Complex **14** adopts a centrosymmetric structure comprised of three dinuclear Au₂ units (total formal charge +6), two dianionic bridging ligands **2S²⁻**, and two monoanionic ligands **2SH⁻** in terminal positions in a ladder-like arrangement to give a neutral complex. As depicted in Fig. 6b (left-hand side), the central Au₂ unit is highly twisted (by *ca.* 90 $^{\circ}$) with respect to the other two Au₂ units. The Au2...Au3 distance of 3.002 Å in **14** is in the middle of the range for Au(I)...Au(I) aurophilic interactions, which are typically 2.50–3.50 Å,²⁰ *e.g.* 3.043(1) Å in [AuS₂P(4-C₆H₄OCH₃)(O-menthyl)]₂²⁴ and 3.018(1) Å in [Au₃(2,6-Me₂-form)₂(THT)Cl] (form = formamidinate).^{25a} However, the central Au1...Au1' distance of 2.874(1) Å is among the shortest observed for such systems^{20,24}.^{Error! Bookmark not defined.} (*cf.* 2.89 Å in cubic close-packed gold metal).²⁰ The tighter Au1...Au1' interaction is reflected in a larger deviation from planarity for the inner gold atoms compared to the other two-coordinate gold centres: \angle S1–Au1–S2 = 167.4(1) $^{\circ}$ vs. N1–Au2–N5 = 171.1(2) $^{\circ}$ and S3–Au3–N2 = 172.0(2) $^{\circ}$.

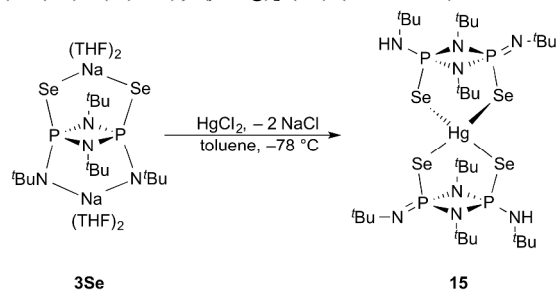
The coordination modes of the ligands in **14** involve *S,S'*, *S'',S'''*-bonding of two dianions **2S²⁻** to the central Au₂ unit, while the terminal Au₂ units are *N,N'*-chelated to a bridging dianion **2S²⁻** and *N,S*-ligated to the terminal monoanionic ligands **2SH⁻**. The Au–S bond lengths of 2.297(6)–2.303(6) Å in the *S,S'*,*S'',S'''*-chelated complex [AuS₂P(4-C₆H₄OCH₃)(O-menthyl)]₂²⁴ are similar to those in **14** (2.288(2)–2.291(2) Å). The Au–N bond lengths of 2.047(6)–2.082(6) Å are also comparable to those found in [Au₃(2,6-Me₂-form)₂(THT)Cl] (2.044(16) Å).^{25a} As expected, the terminal P=S bond distance of 1.939(3) Å in **14** is significantly shorter (by *ca.* 0.11 Å) than the mean value for the three other P–S bonds, which are all engaged in a bridging function.

The ³¹P NMR spectrum of **14** exhibits three distinct resonances: (a) a singlet at 19.2 ppm attributed to the four phosphorus atoms in the centre of the complex on the basis of relative intensity and (b) mutually coupled doublets at 38.1 and 32.9 ppm with a ¹J(P,P) value of 23.4 Hz. The former resonance is tentatively assigned to the P4 atoms by comparison with the value of 38.7 ppm reported for the P=S groups in **1S**.²³

Synthesis, X-ray structure and NMR spectra of a spirocyclic mercury complex

In view of the structure-directing effect of the coinage metal centre in the formation of the products of the reactions of **3Se** with Ag(I) and Au(I) reagents, we decided to investigate the metathesis of this reagent with a halide of a divalent metal that favours linear geometry. The reaction of HgCl₂ with **3Se** in toluene at $-78\text{ }^{\circ}\text{C}$ yielded a variety of products of which the major component (based on the ³¹P NMR spectrum of the reaction mixture), was isolated in 9 % yield and identified as

the homoleptic Hg(II) complex $[\{^t\text{BuN}(\text{Se})\text{P}(\mu\text{-N}^t\text{Bu})_2\text{P}(\text{Se})\text{N}(\text{H}^t\text{Bu})\}_2(\mu\text{-Hg})]$ (**15**) (Scheme 5).



Scheme 5 Synthesis of the spirocyclic mercury complex **15**.

The crystal structure of **15** was elucidated after recrystallisation from *n*-hexane at $-40\text{ }^\circ\text{C}$. The molecular structure is depicted in Fig. 7 together with selected geometrical parameters.

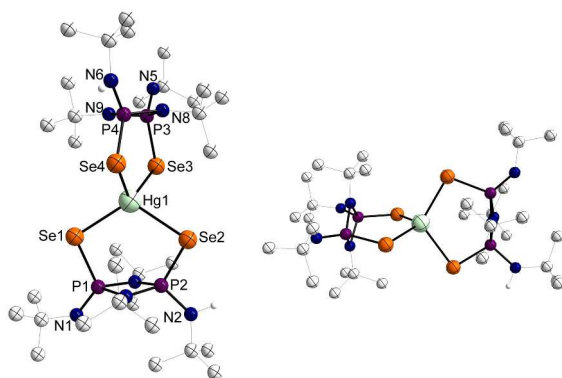


Fig. 7 Two views of the X-ray crystal structure of **15**. Hydrogen atoms bonded to C atoms are omitted for clarity. Selected bond lengths (Å) and bond angles ($^\circ$): Hg1–Se1 2.5969(11), Hg1–Se2 2.7347(11), Hg1–Se3 2.6021(11), Hg1–Se4 2.7373(11), Se1–P1 2.217(3), Se2–P2 2.148(3), Se3–P3 2.212(3), Se4–P4 2.148(3), P1–N1 1.505(9), P2–N2 1.619(8), P3–N5 1.516(9), P4–N6 1.630(8); Se1–Hg1–Se2 113.70(3), Se1–Hg1–Se3 127.23(4), Se1–Hg1–Se4 99.99(3), Se2–Hg1–Se3 96.54(3), Se2–Hg1–Se4 104.43(3), Se3–Hg1–Se4 113.50(3), Hg1–Se1–P1 98.61(7), Hg1–Se2–P2 91.73(7), Hg1–Se3–P3 98.76(8), Hg1–Se4–P4 92.18(7).

Complex **15** is comprised of a spirocyclic Hg^{2+} centre which is *Se,Se'*-chelated by two monoanionic 2SeH^- ligands to give a neutral complex. The distorted tetrahedral geometry around the Hg atom is reflected in the wide range of Se–Hg–Se bond angles ($96.54(3)$ – $127.23(4)^\circ$). Furthermore, the homoleptic complex **15** exhibits two distinct Hg–Se bond distances with mean values of 2.599(1) and 2.736(1) Å, which are associated with the longer and shorter mean P–Se distances of 2.215(3) and 2.148(3) Å, respectively. As observed for the previously discussed complexes of the monoanion 2SeH^- , there is a difference of *ca.* 0.11 Å in the exocyclic P–N bond lengths that can be attributed to the protonation of the N1 and N4 centres. Examples of complexes that exhibit a distorted tetrahedral *Se,Se',Se'',Se'''*-coordination around a Hg(II) centre include $\text{Hg}[\text{HC}(\text{PPh}_2\text{Se})_2]_2$ ²⁶ and $\text{Hg}[(^t\text{Pr}_2\text{PSe})_2\text{N}]_2$.²⁷ The bond lengths in the former complex [$d(\text{Hg}–\text{Se}) = 2.615(1)$ –

2.679(1) Å, $d(\text{P}–\text{Se}) = 2.161(3)$ – $2.197(3)$ Å] are comparable to those found for **15**.²⁶

The ^{31}P NMR spectrum of **15** in toluene at room temperature exhibits two mutually coupled doublets at 4.6 ppm (P2) and -59.2 ppm (P1) with a $^2J(\text{P},\text{P})$ value of 16.3 Hz indicating that there is no proton exchange between nitrogen sites.

Conclusions

The attempted metathetical reactions of the dianion 2Se^{2-} with coinage metal and mercury reagents generated novel macrocyclic and spirocyclic complexes of the corresponding monoprotonated anion 2SeH^- .¹³ Although the isolated yields of **12**, **13** and **15** are low, now that these novel complexes have been structurally identified, the use of the known reagent $[\text{Li}(\text{THF})_2][2\text{SeH}]$ ³⁰ in metathesis with the appropriate metal halide can be expected to enhance the yields substantially.

An interesting structure-directing effect was noted in the outcome of the reactions of **3Se** with Ag(I) and Au(I) reagents. Whereas the trigonal geometry favoured by Ag(I) generates a tetrameric macrocycle with partially bridging ligands (three-coordinate selenium centres), the linear arrangement preferred for Au(I) imposes a trimeric arrangement with only two-coordinate selenium atoms. The latter complex is related to the previously reported trimeric macrocycle **9Se** through the formal insertion of Au atoms into the Se–Se bonds except that none of the exocyclic nitrogen atoms are protonated in the “gold-free” ring.

Complex **14** is the first example containing both 2S^{2-} and 2SH^- ligands and the arrangement of three Au_2 units is unique. Theoretical studies to elucidate the nature of the $\text{Au}\cdots\text{Au}$ interaction are warranted.²⁸ In addition, future experimental investigations should address the photophysical properties of **14** in view of the potential applications of d^{10} gold(I) complexes emanating from their unique photochemical properties.²⁹

Experimental Section

Reagents and general procedures

All synthetic manipulations were performed under an atmosphere of dry argon using standard Schlenk-line techniques and/or a Saffron glove box running with argon unless otherwise stated. All glass apparatus was stored in a drying oven ($120\text{ }^\circ\text{C}$) and flame-dried *in vacuo* (10^{-3} mbar) before use. Dry solvents were collected from an *MBraun* solvent system under a nitrogen atmosphere and stored in Schlenk flasks over 4 Å molecular sieves or were dried and purified using common procedures.³¹ All chemicals were purchased from *Sigma Aldrich* and used without further purification.

Instrumentation

NMR spectra were recorded using a *JEOL DELTA EX 270* or a *BRUKER Avance II 400* spectrometer, a *BRUKER Avance 500* or a *BRUKER Avance III 500* spectrometer. TMS was used as

an internal standard for ^1H NMR. 85 % H_3PO_4 was used as an external standard for $^{31}\text{P}\{^1\text{H}\}$ NMR spectra and Me_2Se for $^{77}\text{Se}\{^1\text{H}\}$ NMR spectra. Chemical shifts (δ) are given in parts per million (ppm) relative to the solvent peaks.³² Coupling constants (J) are given in Hertz (Hz). Mass spectrometry was performed on a *Finnigan MAT 95 XP*, an *Agilent 5975C Inert XL GC/MSD* or a *ThermoFisher LTQ Orbitrap XL* at the EPSRC UK National MS Facility in Swansea. Elemental analysis was performed at the Elemental Analysis Service of the London Metropolitan University (by Mr. S. Boyer).

Preparation of 11

To a suspension of **3Se** (200 mg, 0.24 mmol) in toluene (20 mL) at -78°C a cold (-78°C) toluene solution (15 mL) of $\text{AgCl}(\text{NHC})$ (108 mg, 0.24 mmol) was added dropwise over 15 min by cannula. The reaction mixture was stirred at that temperature for 2 h and then warmed to room temperature, where it was stirred for an additional 20 h. The solvent was removed *in vacuo* and the precipitate was dissolved in *n*-hexane (40 mL), filtered, concentrated and the solution was stored at -40°C overnight. The crystals that formed were removed by filtration and dried *in vacuo*. The filtrate was concentrated and stored at -40°C for another batch of crystals (yield: 12 %). ^{31}P NMR (109.37 MHz, $[\text{D}_8]\text{toluene}$): δ [ppm] = 13.8 (br, $^1J(\text{P,Se}) \approx 714$ Hz), -34.1 (br, $^1J(\text{P,Se}) \approx 650$ Hz). The centres of the broad satellites were taken for the calculation of approximate coupling constants. ^{77}Se NMR (51.52 MHz, $[\text{D}_8]\text{toluene}$): δ [ppm] = 65.5 (d, $^1J(\text{Se,P}) = 647$ Hz), -62.8 (d, $^1J(\text{Se,P}) = 722$ Hz). HR-MS (ESI^+ , m/z), 919.1887 [M^+] (calculated for $\text{C}_{37}\text{H}_{62}\text{P}_2\text{Se}_2\text{N}_6\text{Ag}$: 919.1899 [M^+]). Elemental analysis (%) calcd for $\text{C}_{37}\text{H}_{63}\text{P}_2\text{N}_6\text{AgSe}_2$: C 48.32 H 6.90 N 9.14; found: C 48.22 H 7.02 N 9.07.

Preparation of 12

Procedures were similar to those described for **11** using **3Se** (500 mg, 0.60 mmol) and $\text{Ag}[\text{BF}_4]$ (117 mg, 0.60 mmol). Yield = 22 %. ^1H NMR (400.30 MHz, $[\text{D}_8]\text{toluene}$): δ [ppm] = 3.30 (4H, NH), 1.89 (br, 72H, 2 x ^tBu), 1.78 (br, 36H, ^tBu), 1.23 (br, 36H, ^tBu). ^{31}P NMR (109.37 MHz, $[\text{D}_8]\text{toluene}$): δ [ppm] = 13.9 (br) and -55.4 (br). $^1J(\text{P,Se})$ could not be determined due to broad signals. HR-MS (ESI^+ , m/z), 614.9943 [$M^+\text{+H}$] (calculated for a monomer unit $\text{C}_{16}\text{H}_{38}\text{P}_2\text{N}_4\text{Se}_2\text{Ag}$: 614.9953 [$M^+\text{+H}$]). Elemental analysis (%) calcd for $\text{C}_{64}\text{H}_{148}\text{P}_8\text{N}_{16}\text{Ag}_4\text{Se}_8$: C 31.34 H 6.08 N 9.14 found: C 31.26 H 6.00 N 9.03.

Preparation of 13

Procedures were similar to those described for **11** using **3Se** (500 mg, 0.60 mmol) and $\text{AuCl}(\text{THT})$ (192 mg, 0.60 mmol). Total yield of red crystals = 14 %. The ^{31}P NMR spectrum of the filtrate revealed additional amounts of **13** that could not be separated from the by-product **1Se**. ^1H NMR (400.30 MHz,

$[\text{D}_8]\text{toluene}$): δ [ppm] = 3.85 (3NH), 1.93 (54H, 2 x ^tBu), 1.52 (27H, ^tBu) 1.22 (27H, ^tBu). ^{31}P NMR (109.37 MHz, $[\text{D}_8]\text{toluene}$): δ [ppm] = 4.9 (d, $^1J(\text{P,Se}) = 657$ Hz, $^2J(\text{P,P}) = 16.4$ Hz), -57.6 (d, $^1J(\text{P,Se}) = 627$ Hz, $^2J(\text{P,P}) = 16.4$ Hz). ^{77}Se NMR (51.52 MHz, $[\text{D}_8]\text{toluene}$): δ [ppm] = 132.4 (d, $^1J(\text{P,Se}) = 621$ Hz), 209.0 (d, $^1J(\text{P,Se}) = 644$ Hz). MS (EI^+ , m/z), 648.9 [$^{1/3}M^+$] (calcd: 649.0 [$^{1/3}M^+ = \text{C}_{16}\text{H}_{38}\text{Au}_1\text{P}_2\text{Se}_2$]). Accurate elemental analyses could not be obtained owing to a minor contamination of the product with $\text{AuCl}(\text{THT})$.

Preparation of 14

Procedures were similar to those described for **11** using **3S** (500 mg, 0.68 mmol) and $\text{AuCl}(\text{THT})$ (216 mg, 0.68 mmol). Yield of colourless crystals = 49 %. ^1H NMR (400.30 MHz, $[\text{D}_8]\text{toluene}$): δ [ppm] = (signals for NH could not be reliably identified) 1.87 (36H, 4 x ^tBu), 1.83 (36H, 4 x ^tBu), 1.67 (18H, 2 x ^tBu), 1.51 (36H, 4 x ^tBu), 1.36 (18H, 2 x ^tBu). ^{31}P NMR (109.37 MHz, $[\text{D}_8]\text{toluene}$): δ [ppm] = 38.1 (d, $^2J(\text{P,P}) = 23.4$ Hz), 32.9 (d, $^2J(\text{P,P}) = 23.4$ Hz), 19.2 (s). Elemental analysis (%) calcd for $\text{C}_{64}\text{H}_{146}\text{P}_8\text{N}_{16}\text{Au}_6\text{S}_8$: C 27.20 H 5.21 N 7.93 found: C 27.46 H 5.02 N 7.73.

Preparation of 15

Procedures were similar to those used for **11** using **3Se** (500 mg, 0.60 mmol) and HgCl_2 (163 mg, 0.60 mmol). Total yield of colourless crystals: 9 %. ^1H NMR (400.30 MHz, $[\text{D}_8]\text{toluene}$): δ [ppm] = (signals for NH could not be reliably identified) 1.94 (^tBu), 1.75 (^tBu), 1.62 (^tBu), 1.58 (^tBu). ^{31}P NMR (109.37 MHz, $[\text{D}_8]\text{toluene}$): δ [ppm] = 4.6 (d, $^2J(\text{P,P}) = 16.3$ Hz), -59.2 (d, $^2J(\text{P,P}) = 16.3$ Hz). $^1J(\text{P,Se})$ could not be determined due to the weak intensity of the resonances. HR-MS (ESI^+ , m/z), 1213.1454 [$M^+\text{+H}$] (calculated for $\text{C}_{32}\text{H}_{75}\text{P}_4\text{Se}_4\text{N}_8\text{Hg}$: 1213.1448 [$M^+\text{+H}$]). Elemental analysis (%) calcd for $\text{C}_{32}\text{H}_{74}\text{P}_4\text{N}_8\text{HgSe}_4$: C 31.73 H 6.16 N 9.25 found: C 31.44 H 6.28 N 9.15.

Crystal structure determinations

X-ray analysis for **11-15** were performed using a Rigaku FRX (dual port) rotating anode/confocal optic high brilliance generator with Dectris P200 detectors, and Oxford Cryostream Cobra accessory at $-180(1)^\circ\text{C}$. All data were collected with Mo-K α radiation ($\lambda = 0.71073 \text{ \AA}$) and corrected for Lorentz and polarisation effects. The data for all of the compounds were collected and processed using *CrystalClear (Rigaku)*.³³ The crystal structures were solved using direct methods³⁴ or heavy-atom Patterson methods³⁵ and expanded using Fourier techniques.³⁶ The non-hydrogen atoms were refined anisotropically, hydrogen atoms were refined using the riding model. All calculations were performed using *CrystalStructure*³⁷ crystallographic software package and *SHELXL-97*.³⁸

Table 1 X-ray crystallographic data for compounds **11-15**.

	11	12	13	14	15
--	----	----	----	----	----

Empirical formula	C ₃₇ H ₆₁ AgN ₆ P ₂ Se ₂	C ₆₆ H ₁₅₂ Ag ₄ N ₁₆ O ₅ P ₈ Se ₈	C ₄₈ H ₁₁₁ Au ₃ N ₁₂ P ₆ S ₆	C ₆₄ H ₁₄₆ Au ₆ N ₁₆ P ₈ S ₈	C ₃₂ H ₇₄ HgN ₈ P ₄ Se ₄
Formula weight	917.66	2488.98	2106.99	2826.03	1211.32
Temperature (°C)	93	93	93	93	93
Crystal colour, habit	colourless platelet	colourless prism	pink prism	colourless prism	colourless prism
Crystal dimensions (mm ³)	0.20 x 0.10 x 0.03	0.20 x 0.20 x 0.18	0.12 x 0.03 x 0.03	0.20 x 0.10 x 0.10	0.10 x 0.10 x 0.10
Crystal system	monoclinic	monoclinic	hexagonal	orthorhombic	tetragonal
<i>a</i> (Å)	16.921(6)	14.449(3)	20.606(2)	31.316(4)	28.096(3)
<i>b</i> (Å)	14.566(5)	27.568(6)	20.606(2)	18.931(2)	28.096(3)
<i>c</i> (Å)	17.507(6)	25.838(6)	10.6403(11)	17.846(2)	16.694(2)
α (°)	90.0000	90.0000	90.0000	90.0000	90.0000
β (°)	94.846(10)	94.091(5)	90.0000	90.0000	90.0000
γ (°)	90.0000	90.0000	120.0000	90.0000	90.0000
Volume (Å ³)	4300(3)	10266(4)	3912.5(7)	10580(2)	13178(3)
Space group	<i>P</i> 2 ₁ / <i>n</i>	<i>P</i> 2 ₁ / <i>n</i>	<i>P</i> 63/ <i>m</i>	<i>P</i> bcn	<i>P</i> 4/ <i>n</i>
<i>Z</i> value	4	4	2	4	8
<i>D</i> _{calc} (g/cm ³)	1.417	1.610	1.788	1.774	1.221
<i>F</i> ₀₀₀	1880.00	4976.00	2028.00	5456.00	4784.00
μ (Mo- <i>K</i> α) (cm ⁻¹)	2.267	3.754	8.581	8.637	4.672
No. of reflections measured	54874	124373	53212	134200	134164
<i>R</i> _{int}	0.1066	0.1067	0.0455	0.0461	0.1243
Min. and max. transmissions	0.569, 0.934	0.326, 0.509	0.488, 0.773	0.275, 0.422	0.404, 0.627
Reflection/parameter ratio	7654 (451)	18691 (994)	2519 (137)	9658 (484)	12081 (466)
Residuals: <i>R</i> ₁ (<i>I</i> > 2.00 σ (<i>I</i>))	0.0874	0.0753	0.0571	0.0339	0.0575
Residuals: <i>wR</i> ₂ (all reflections)	0.2517	0.2208	0.1676	0.1105	0.2089
Goodness of fit indicator	1.034	1.141	1.080	1.045	1.038
Maximum peak in final diff. map (e ⁻ /Å ³)	1.48	2.21	2.63	3.81	3.68
Minimum peak in final diff. map (e ⁻ /Å ³)	-1.30	-0.83	-3.49	-1.73	-1.19
CCDC number	1042701	1042702	1042703	1042704	1042700

Acknowledgements

Financial support from the EPSRC and NSERC (Canada) is gratefully acknowledged.

Notes and references

^a School of Chemistry, University of St Andrews, St Andrews KY16 9ST, Scotland.

^b Department of Chemistry, University of Calgary, Calgary, AB, Canada T2N 1N4.

† Electronic Supplementary Information (ESI) available: X-ray structure of **10** and packing diagrams for **12**, **13** and **14**. Crystallographic details CCDC 1042700-1042704 for **11**, **12**, **13**, **14** and **15**. See DOI: 10.1039/c000000x/

- 1 T. Chivers and I. Manners, *Inorganic Rings and Polymers of the p-Block Elements: From Fundamentals to Applications*, Royal Society of Cambridge, 2009.
- 2 For reviews, see (a) M. S. Balakrishna, D. J. Eisler and T. Chivers, *Chem. Soc. Rev.*, 2007, **36**, 650; (b) L. Stahl, *Coord. Chem. Rev.*, 2000, **210**, 203; (c) M. S. Balakrishna, V. S. Reddy, S. S. Krishnamurthy, J. F. Nixon and J. C. T. R. St. Laurent, *Coord. Chem. Rev.*, 1994, **129**, 1; (d) R. Keat, *Top. Curr. Chem.*, 1982, **102**, 89.

- 3 For a recent review, see S. G. Calera and D. S. Wright, *Dalton Trans.*, 2010, **39**, 5055, and references cited therein.
- 4 S. G. Calera, D. J. Eisler, J. M. Goodman, M. McPartlin, S. Singh and D. S. Wright, *Dalton Trans.*, 2009, 1293.
- 5 S. G. Calera, D. J. Eisler, J. V. Morey, M. McPartlin, S. Singh and D. S. Wright, *Angew. Chem., Int. Ed.*, 2008, **47**, 1111.
- 6 M. M. Siddiqui, S. M. Mobin, I. Senkovska, S. Kaskel and M. S. Balakrishna, *Chem. Commun.*, 2014, **50**, 12273.
- 7 M. S. Balakrishna, *J. Organomet. Chem.*, 2010, **695**, 925, and references cited therein.
- 8 (a) G. G. Briand, T. Chivers and M. Krahn, *Coord. Chem. Rev.*, 2002, **233-234**, 237; (b) T. Chivers, M. Krahn and M. Parvez, *Chem. Commun.*, 2000, 463.
- 9 T. Chivers, C. Fedorchuk, M. Krahn, M. Parvez and G. Schatte, *Inorg. Chem.*, 2001, **40**, 1936.
- 10 A. Nordheider, T. Chivers, R. Thirumoorthi, I. Vargas-Baca and J. D. Woollins, *Chem. Commun.*, 2012, **48**, 6346.
- 11 (a) D. Aris, J. Beck, A. Decken, I. Dionne, J. Schmedt auf der Günne, W. Hoffbauer, T. Köchner, I. Krossing, J. Passmore, E. Rivard, F. Steden and X. Wang, *Dalton Trans.*, 2011, **40**, 5865 (b) T. Köchner, N. Trapp, T. A. Engesser, A. J. Lehner, C. Röhr, S. Riedel, C. Knapp, H. Scherer and I. Krossing, *Angew. Chem., Int. Ed.*, 2011, **50**, 11253; (c) J. Schaeffer, A. Steffani,

- D. A. Plattner and I. Crossing, *Angew. Chem., Int. Ed.*, 2012, **51**, 6009.
- 12 A. Nordheider, PhD thesis, University of St Andrews, 2014. For details of the X-ray structure of $[\text{Ag}(\mathbf{1Se})_2][\text{CF}_3\text{SO}_3]$ (**10**) see ESI, CCDC 1042705.
- 13 In earlier investigations the formation of the diprotonated precursors **1Se** [$\delta(^{31}\text{P}) = 26.7$ ppm, $^1J(\text{P},\text{Se}) = 880$ Hz) and **1S** ($\delta(^{31}\text{P}) = 40.0$ ppm) was proposed to be the result of a radical process. Semi-empirical MO calculations of the model system $[\text{Me}(\text{H})\text{N}(\text{S})\text{P}(\mu\text{-NMe})_2\text{P}(\text{S})\text{NMe}]^+$ indicate a nitrogen-based SOMO (spin population at nitrogen = 0.957) instead of the formation of a sulfur-based radical which would dimerise to form a S–S bond. Thus, in addition to metathesis, reactions of 2Se^{2-} and 2S^{2-} may involve partial oxidation to produce nitrogen-based radicals that rapidly abstract hydrogen atoms from the solvent (THF or toluene) to form **1Se** and **1S**. This suggestion was confirmed by EPR studies and the formation of **1S** in the reaction of Li_3SH with TeCl_4 . G. G. Briand, T. Chivers and G. Schatte, *Inorg. Chem.*, 2002, **41**, 1958.
- 14 H. Liu, N. A. G. Bandeira, M. J. Calhorda, M. G. B. Drew, V. Felix, J. Novosad, F. F. de Biani and P. Zanello, *J. Organomet. Chem.*, 2004, **689**, 2808.
- 15 T. Chivers, M. Krahn and G. Schatte, *Inorg. Chem.*, 2002, **41**, 4348.
- 16 A. Cingolani, Effendy, M. Pellei, C. Pettinari, C. Santini, B. W. Skelton and A. H. White, *Inorg. Chem.*, 2002, **41**, 6633.
- 17 M. C. Copsey, A. Panneerselvam, M. Afzaal, T. Chivers and P. O'Brien, *Dalton Trans.*, 2007, 1528.
- 18 A. Burini, A. A. Mohamed and J. P. Fackler, Jr., *Comments Inorg. Chem.*, 2003, **24**, 253.
- 19 M. N. Pillay, B. Omondi, R. J. Staples and W. E. van Zyl, *CrystEngChem.*, 2013, **15**, 4417.
- 20 H. Schmidbaur and A. Schier, *Chem. Soc. Rev.*, 2012, **41**, 370.
- 21 *The Cambridge Structural Database: a quarter of a million crystal structures and rising*, F. H. Allen, *Acta Crystallogr.*, 2002, **B58**, 380.
- 22 P. G. Jones and C. Thöne, *Inorg. Chim. Acta*, 1991, **181**, 291.
- 23 T. G. Hill, R. C. Haltiwanger, M. L. Thompson, S. A. Katz and A. D. Norman, *Inorg. Chem.*, 1994, **33**, 1770.
- 24 W. E. van Zyl, J. M. López-de-Luzuriaga, A. A. Mohamed, R. J. Staples and J. P. Fackler, Jr., *Inorg. Chem.*, 2002, **41**, 4579.
- 25 (a) H. E. Abdou, A. A. Mohamed and J. P. Fackler, Jr., *Inorg. Chem.*, 2005, **44**, 166; (b) A. Maspero, I. Kani, A. A. Mohamed, M. A. Omary, R. J. Staples and J. P. Fackler, Jr., *Inorg. Chem.*, 2003, **42**, 5311.
- 26 J. Konu, H. M. Tuononen and T. Chivers, *Inorg. Chem.*, 2009, **48**, 11788.
- 27 D. J. Crouch, P. M. Hatton, M. Helliwell, P. O'Brien and J. Raftery, *Dalton Trans.*, 2003, 2761.
- 28 P. Pyykkö, *Chem. Soc. Rev.*, 2008, **37**, 1967, and references therein.
- 29 (a) V. W.-W. Yam and E. C.-C. Cheng, *Chem. Soc. Rev.*, 2008, **37**, 1806; (b) S. Bestgen, M. T. Gamer, S. Lebedkin, M. M. Kappes and P. W. Roesky, *Chem. Eur. J.*, DOI: 10.1002/chem.201404985 and references cited therein.
- 30 T. Chivers, M. Krahn, M. Parvez and G. Schatte, *Inorg. Chem.*, 2001, **40**, 2547.
- 31 D. D. Perrin and W. L. F. Armarego, *Purification of Laboratory Chemicals*, Oxford, Butterworth-Heinemann, 6th edn., 2009.
- 32 G. R. Fulmer, A. J. M. Miller, N. H. Sherden, H. E. Gottlieb, A. Nudelman and B. M. Stoltz, *Organometallics*, 2010, **29**, 2176.
- 33 (a) CrystalClear 1.6: Rigaku Corporation, 1999; (b) CrystalClear Software User's Guide, Molecular Structure Corporation[®], 2000; (c) J. W. Pflugrath, *Acta Crystallogr.*, 1999, **D55**, 1718.
- 34 SIR97: A. Altomare, M. Burla, M. Camalli, G. Cascarano, C. Giacovazzo, A. Guagliardi, A. Moliterni, G. Polidori and R. Spagna, *J. Appl. Crystallogr.*, 1999, **32**, 115.
- 35 PATTY: P. T. Beurskens, G. Admiraal, H. Behm, G. Beurskens, J. M. M. Smits and C. Smykalla, *Z. Kristallogr.*, 1991, **Suppl. 4**, 99.
- 36 DIRDIF99: P. T. Beurskens, G. Admiraal, G. Beurskens, W. P. Bosman, R. de Gelder, R. Israel and J. M. M. Smits, The DIRDIF-99 program system, Technical Report of the Crystallography Laboratory, University of Nijmegen, The Netherlands, 1999.
- 37 (a) CrystalStructure 3.8.1: Crystal Structure Analysis Package, Rigaku and Rigaku/MS (2000–2006). 9009 New Trails Dr. The Woodlands, TX 77381 USA; (b) CrystalStructure 4.0: Crystal Structure Analysis Package, Rigaku Corporation (2000–2010). Tokyo 196-8666, Japan.
- 38 G. M. Sheldrick, *Acta Crystallogr.*, 2008, **A64**, 112.

ARTICLE

TOC entry

Reactions of the dianions $[\text{tBuN}(\text{E})\text{P}(\mu\text{-N}'\text{Bu})_2]^{2-}$ ($\text{E} = \text{Se}, \text{S}$) with $\text{M}(\text{I})$ reagents ($\text{M} = \text{Ag}, \text{Au}$) or HgCl_2 produce complexes that incorporate the corresponding monoanions $[\text{tBu}(\text{H})\text{N}(\text{E})\text{P}(\mu\text{-N}'\text{Bu})_2\text{P}(\text{E})\text{N}'\text{Bu}]^-$ in spirocyclic, macrocyclic or ladder structures.

